Insulin-like Growth Factor-I–Dependent Up-regulation of ZEB1 Drives Epithelial-to-Mesenchymal Transition in Human Prostate Cancer Cells

Tisheeka R. Graham,[1] Haiyen E. Zhau,[2] Valerie A. Odero-Marah,[6] Adeboye O. Osunkoya,[3] K. Sean Kimbro,[1] Mourad Tighiouart,[4] Tongrui Liu,[1] Jonathan W. Simons,[1,5,7] and Ruth M. O'Regan[1]

[1]Department of Hematology and Oncology, Winship Cancer Institute, Departments of [2]Molecular Urology and Therapeutics, [3]Pathology and Urology, [4]Biostatistics, and [5]Biomedical Engineering, Emory University; [6]Department of Biological Sciences, Clark Atlanta University; [7]Department of Material Sciences Engineering, Georgia Institute of Technology, Atlanta, Georgia

Abstract

The epithelial-to-mesenchymal transition (EMT) is crucial for the migration and invasion of many epithelial tumors, including prostate cancer. Although it is known that ZEB1 overexpression promotes EMT primarily through down-regulation of E-cadherin in a variety of cancers, the soluble ligands responsible for the activation of ZEB1 have yet to be identified. In the present study, we investigated the role of insulin-like growth factor-I (IGF-I) in the regulation of ZEB1 during EMT associated with prostate tumor cell migration. We found that ZEB1 is expressed in highly aggressive prostate cancer cells and that its expression correlates directly with Gleason grade in human prostate tumors ($P < 0.001$). IGF-I up-regulates ZEB1 expression in prostate cancer cells exhibiting an epithelial phenotype. In prostate cancer cells displaying a mesenchymal phenotype, ZEB1 inhibition reverses the suppression of E-cadherin protein and down-regulates the expression of the mesenchymal markers N-cadherin and fibronectin. Furthermore, ZEB1 blockade decreases migratory and invasive potential in $ARCaP_M$ compared with the control. These results identify ZEB1 as a key transcriptional regulator of EMT in prostate cancer and suggest that the aberrant expression of ZEB1 in prostate cancer cells occurs in part in response to IGF-I stimulation. [Cancer Res 2008;68(7):2479–88]

Introduction

Prostate cancer is the second leading cause of cancer-related mortality in men in the United States (1). Androgen ablation therapy is an effective treatment for hormone-dependent prostate cancer; however, a subset of patients ultimately develops hormone-refractory disease. Therefore, there is a need to identify and characterize important regulators of aggressive prostate cancers. Many of these aggressive cancers recapitulate normal developmental processes, such as the epithelial-to-mesenchymal transition (EMT), to enhance cell migration and invasion. The conversion of an epithelial cell into a mesenchymal cell requires alterations in morphology, cellular architecture, adhesion, and migration (2, 3). There is mounting evidence that the acquisition of migratory and invasive properties by epithelial cells occurs in response to the microenvironment, which is associated with gain of mesenchymal and loss of epithelial characteristics (3, 4). In addition, cells in the center of a prostate cancer maintain an epithelial phenotype, whereas cells at the invasive front have a mesenchymal phenotype characterized by increased expression of mesenchymal markers (5). There is increased expression of transcription factors, such as Snail, Slug, Twist, E47, ZEB1, and ZEB2, which leads to increased expression of N-cadherin and vimentin and concomitant decrease of E-cadherin and cytokeratins, proteins essential for establishment of cell-cell adhesion (4, 6–8).

ZEB1 (zinc finger enhancer binding protein; also known as ZFHX1A, AREB6, or δEF1) is a zinc finger homeodomain transcriptional repressor that regulates developmental processes such as skeletal patterning and muscle and lymphoid differentiation (9). ZEB1 and the related gene *ZEB2* were first isolated from a *Drosophila* cDNA expression library (10). Both proteins contain two C2H2 (Kruppel)-type zinc finger clusters at their COOH and NH_2 termini as well as central homeobox domain (11, 12). Despite the high homology and the identical overall gene structure of ZEB1 and ZEB2, there are differences in their pattern of expression and repressor domain organization (10, 12). ZEB1 also regulates EMT in breast, uterine, and colorectal cancers (8, 13–15). ZEB1 represses E-cadherin through interaction with a CANNTG sequence (named E-box) in the promoter region and further recruitment of histone deacetylase 1 leading to chromatin condensation and gene silencing (14, 16, 17). E-cadherin loss is linked to increased tumor migration and invasion both *in vitro* and *in vivo* (18–20). ZEB1 can act as a transcriptional repressor or activator depending on several poorly understood conditions (21).

The insulin-like growth factor (IGF) axis plays an important role in regulating cell growth, proliferation, survival, and metabolism. IGF-I, a 7.7-kDa peptide, is both a systemic and local growth factor (22). IGF-I assumes an important role in both normal and neoplastic growth (23). The IGF axis consists of two ligands (IGF-I and IGF-II), two surface receptors (IGF-IR and IGF-IIR), six binding proteins (IGFBP-1 to IGFBP-8) that regulate the availability to the receptors, and a group of IGFBP proteases that cleave IGFBP and modulate the action of IGFs (24). IGF-I binds to IGF-IR and the tyrosine kinase on the cytoplasmic domain of IGF-IR transduces IGF-I signaling into cells (24, 25). Multiple signaling proteins are activated downstream of these receptors, including the extracellular signal-related kinase (ERK)/mitogen-activated protein kinase (MAPK), phosphatidylinositol 3′-kinase (PI3K), and Akt. IGF-I signaling has been implicated in a variety of human cancers and promotes tumorigenesis (25). There is growing evidence suggesting

Requests for reprints: Ruth M. O'Regan, Winship Cancer Institute, Emory University School of Medicine, 1701 Uppergate Drive, WCI Building C, Atlanta, GA 30322. Phone: 404-778-5994; Fax: 404-778-5530; E-mail: Ruth.ORegan@emoryhealthcare.org.

doi:10.1158/0008-5472.CAN-07-2559

that IGF-I is involved in the development of prostate cancer because there are elevated levels of IGF-I in the serum of patients with this disease (26, 27). Additionally, the majority of prostate cancers express the IGF-IR, and IGF-I has been found to be one of the most potent mitogens to prostate cancer cells *in vitro* (28, 29). Androgen-independent prostate cancer cells have increased expression of IGF-I and IGF-IR compared with androgen-dependent cells (30, 31).

IGF-I is not only secreted from the cancer cells but is also synthesized by stromal cells (32), soft tissues, and bone, where it can function in an autocrine and paracrine manner (33, 34). This soluble ligand may increase the metastatic potential of prostate cancer by participating in EMT. Irie et al. (35) investigated the effects of IGF-I stimulation on IGF-IR stably transfected breast cancer cells MCF-10A and observed that IGF-I induced a conversion from a cuboidal, epithelial morphology to a more spindle-shaped morphology. In addition, there was repression of E-cadherin and induction of N-cadherin expression on IGF-I stimulation (35). Based on these findings and previous reports linking IGF-I to prostate cancer progression and the essential role of ZEB1 in promoting EMT, we investigated the mode of IGF-I action on ZEB1 expression in the androgen refractory carcinoma of the prostate (ARCaP) cell model. The $ARCaP_E$ cells (E = epithelial) express low levels of endogenous ZEB1 compared with the $ARCaP_M$ (M = mesenchymal), which had elevated expression of ZEB1. IGF-I increased the mRNA and protein levels of ZEB1 in $ARCaP_E$ cells to levels comparable with $ARCaP_M$ and also elevated the expression of the mesenchymal markers N-cadherin and fibronectin. Moreover, small interfering RNA (siRNA) strategy in $ARCaP_M$ cells resulted in an up-regulation of E-cadherin and suppression of mesenchymal markers. To date, there are no reports characterizing ZEB1 in prostate cancer EMT, and the mechanism(s) by which it influences different cellular processes remains unresolved. We propose that ZEB1 is a key mediator of prostate cancer EMT due to its regulation by IGF-I.

Materials and Methods

Cell lines and culture. $ARCaP_E$ and $ARCaP_M$ cell lines were generously donated by Dr. Leland W.K. Chung (Emory University, Atlanta, GA). LNCaP and C4-2B, the androgen-independent subline of LNCaP, were donated by Dr. Leland W.K. Chung. PC-3 and DU-145 cells were purchased from the American Type Culture Collection and cultured as described in T-medium (Invitrogen) supplemented with 5% fetal bovine serum (FBS).

Antibodies and reagents. The rabbit and goat polyclonal ZEB1 (H-102 and E-20), mouse polyclonal vimentin, and transcription factor IID (TFIID) antibodies were purchased from Santa Cruz Biotechnology. The mouse monoclonal E-cadherin, N-cadherin, and fibronectin antibodies were purchased from BD Transduction Laboratories. Treatment of cells with IGF-I was done using LongR^{3}IGF-I (Diagnostic Systems Laboratories), which exhibits relatively low affinity for the IGF-binding proteins. The MAPK/ERK kinase (MEK) inhibitor U0126, rabbit polyclonal phosphorylated and total IGF-IRβ, phosphorylated and total p42/p44, and β-catenin antibodies were obtained from Cell Signaling Technology.

RNA preparation and semiquantitative reverse transcription-PCR. Cells were grown to reach 70% to 80% confluence and serum starved for 24 h before the addition of recombinant IGF-I. Total RNA was harvested using Qiagen RNeasy RNA extraction kit. cDNA was synthesized from $ARCaP_E$ and $ARCaP_M$ cells treated with recombinant IGF-I or from a panel of prostate cancer cell lines using the SuperScript First-Strand cDNA Synthesis kit (Invitrogen). cDNAs were used for PCR analysis using the following oligonucleotide primers: ZEB1: forward, 5′-TTCAGCATCACCAGGCAGTC-3′ and reverse, 5′-GAGTGGAGGAGGCTGAGTAG-3′ (the PCR conditions were as follows: 40 cycles at 94°C for 30 s, annealing at 53°C for 30 s, extension at 72°C for 2 min, and a final extension at 72°C for 7 min); 28S rRNA: forward, 5′-ACGGTAACGCAGGTGTCCT-3′ and reverse, 5′-CCTCTCGTACTGAGCAGGA-3′ (the PCR conditions were as follows: 29 cycles at 95°C for 40 s, annealing at 56°C for 30 s, extension for 1 min, and a final extension at 72°C for 7 min). PCRs were run on a 2% agarose gel. Bands were visualized under UV illumination followed by densitometric analysis using ImageJ software[8] (NIH, Bethesda, MD).

Immunoblot analysis. Cells were lysed in a modified radioimmunoprecipitation assay buffer: 1 mol/L Tris, 5 mol/L NaCl, 1% Triton X-100, 1 mmol/L sodium orthovanadate, and protease inhibitor cocktail (Roche). The lysates were freeze thawed thrice followed by a spin at 13,000 × *g* for 30 min at 4°C. For cytosolic and nuclear fractions, the cells were resuspended in a hypotonic buffer [10 mmol/L Tris (pH 7.5), 1.5 mmol/L $MgCl_2$, 10 mmol/L KCl, 1 mmol/L DTT, pepstatin, leupeptin] and homogenized using a glass douncer. The cells were centrifuged at 13,000 rpm and the supernatant was collected (cytosolic fraction). The nuclei were resuspended in a high salt buffer [20 mmol/L HEPES (pH 7.9), 25% glycerol, $MgCl_2$, 1.2 mol/L KCl, 0.2 mmol/L EDTA, 0.2 mmol/L phenylmethylsulfonyl fluoride, 1 mmol/L DTT] and rotated at 4°C. Cell lysates were quantitated using bicinchoninic acid protein assay reagents (Pierce). Total protein (30 μg) was separated by SDS-PAGE (10%) and transferred onto a polyvinylidene difluoride membrane (Bio-Rad). The membranes were blocked in 5% nonfat dry milk diluted in TBST [0.2 mol/L NaCl, 10 mmol/L Tris (pH 7.4), 0.2% Tween 20] for 1 h at room temperature and then incubated with primary antibodies overnight at 4°C. The following day, the membranes were washed with TBS containing 0.2% Tween 20, and the membranes were subsequently incubated with horseradish peroxidase–labeled secondary antibodies for 1 h at room temperature followed by washing with TBST. The signal was detected by incubation with enhanced chemiluminescence reagents (Amersham Pharmacia Biotech) and exposed on HyBlot CL autoradiography film (Denville Scientific). To assess sample loading, the membrane was stripped with Restore Western Blot Stripping Buffer (Pierce) and probed with a β-actin antibody. Images were resized using Adobe Photoshop software.

Small interfering RNA. $ARCaP_M$ cells were seeded in six-well plates in 5% FBS containing T-medium. The following day, when the cells reached 80% confluency, 200 nmol/L siRNA for either ZEB1 or control (lamin A or cyclophilin B) was transfected using TransIT-TKO transfection reagent following the manufacturers' instructions (Mirus). The siRNA against cyclophilin B, lamin A, and ZEB1 was purchased from Dharmacon RNA Technologies. Forty-eight hours after transfection, whole-cell lysates were prepared as described above.

Transient transfection. The human ZEB1 cDNA cloned into pPCR-BluntII-TOPO was purchased from Open Biosystems. A *Xba*I/*Bam*HI digest removed the human ZEB1 cDNA from pPCR-BluntII-TOPO and was subcloned into pFlagC1 to generate pFlagC1-ZEB1. This construct was sequenced from the 5′ and 3′ ends to verify the presence and identity of the insert. $ARCaP_E$ cells were grown to 80% confluency and transfected with 2.5 μg of control plasmid (pFlagC1) or ZEB1 expression vector (pFlagC1-ZEB1) using Lipofectamine 2000 (Invitrogen). Forty-eight hours after transfection, the whole-cell lysate was harvested and used for immunoblot analysis.

Scratch wound assay. $ARCaP_M$ and $ARCaP_E$ cells were cultured in T-medium containing 5% FBS in a six-well dish. Once the cells were fully confluent, they were serum starved overnight. The following day, a uniform scratch was made down the center of the well using a micropipette tip followed by washing with 1× PBS. Vehicle, recombinant IGF-I (200 ng/mL) was added to the respective wells. To determine the role ZEB1 has on prostate cancer cell migration, $ARCaP_M$ cells were transfected with ZEB1 siRNA or cyclophilin B siRNA for 48 h before the induction of the scratch. The speed of the wound closure was monitored at the indicated time points. Photographic imaging was taken using the Olympus 1X50 inverted microscope.

Immunofluorescence. $ARCaP_M$ cells were transfected with either ZEB1 siRNA or cyclophilin B siRNA for 72 h before immunostaining followed by

[8] http://rsb.info.nih.gov/ij/

fixation with methanol for 5 min at −20°C. The cells were subsequently blocked with 5% goat serum diluted in 1× PBS for 1 h at room temperature and incubated with an antibody against E-cadherin (1:100 in 5% goat serum) for 1 h at room temperature. The cells were washed with PBS-Tween 20 (0.1%) followed by FITC-labeled secondary antibody (Zymed) or Alexa Fluor 555 (1:250 in 5% goat serum; Invitrogen) for 1 h at room temperature. The cells were counterstained with 4′,6-diamidino-2-phenylindole. Following washing, slides were rinsed in water and mounted with Biomeda M01 gel mount. Images were captured with the Zeiss Axioplan 2 upright fluorescence microscope using the Axiovision 4.5 software (Zeiss).

Immunohistochemical analysis of tissue microarrays. The prostate cancer tissue microarrays were purchased from US Biomax. Detection of ZEB1 of normal and prostate tumor tissue specimens was conducted using Dako Autostainer Plus System (Dako Corp.). Tissues were deparaffinized, rehydrated, and subjected to 5-mn pressure cooking antigen retrieval at 125°C and 20 p.s.i. for 30 s; 10-min double endogenous enzyme block, 4°C overnight incubation with primary antibody against ZEB1 (E-20, 4 μg/mL); and 15-min each of biotinylated link and streptavidin-peroxidase reagent incubation. Signals were detected by adding substrate hydrogen peroxide using diaminobenzidine as chromogen and counterstained by hematoxylin. All reagents were obtained from Dako. Goat serum was used as negative control. The cores were scored by a pathologist as negative (0), weak (1), moderate (2), or strong (3) for ZEB1. Statistical analysis was performed using the Fisher's exact test.

Matrigel invasion chamber assay. Invasion assays were performed using Boyden chambers containing polycarbonate inserts of 8-μm pore size membranes. The inserts were coated with 1:4 diluted Matrigel basement membrane matrix (BD Biosciences). $ARCaP_M$ cells (5×10^4) were transfected with ZEB1 or cyclophilin B siRNA. The cells were seeded in quadruplicates in the top well of the inserts in RPMI 1640 containing 5% charcoal-stripped FBS. After 24 h of incubation, cells that invaded through the Matrigel were fixed with formaldehyde, stained with 0.5% crystal violet, and counted to obtain relative invasion. Each condition was performed in quadruplicate and the average number of cells per field is represented.

Statistical analysis. All data are representatives of two or three independent experiments with similar results. Statistical analysis was done using Microsoft Excel software. Significant differences were analyzed using Student's *t* test and two-tailed distribution. A *P* value of <0.005 was deemed significant. Error bars in histograms represent the SD between triplicate experiments. The analysis of the association between ZEB1 expression levels and Gleason scores for prostate cancer was done using Fisher's exact test 4 by 3 contingency table.

Results

Endogenous ZEB1 expression in prostate cancer cells. In this study, we used the ARCaP cell models. ARCaP cells were initially described by Xu et al. (36) as immortalized prostate cancer cells of

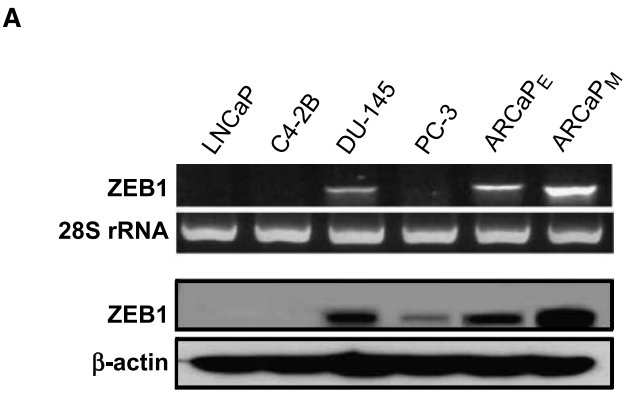

C

ZEB1 Expression in Normal, Low Gleason and High Gleason Score Prostate Carcinomas			
ZEB1	Normal *n* = 17	Low Gleason *n* = 13	High Gleason *n* = 60
No (Score=0)	10	1	
Weak (Score=1)	7	10	
Moderate (Score=2)		2	15
Strong (Score=3)			45

Figure 1. Differential expression of ZEB1 in prostate cancer cell lines and tissues. *A,* semiquantitative RT-PCR analysis and Western blot analysis were used to compare the mRNA level and protein levels of ZEB1 in LNCaP, C4-2B, DU-145, PC-3, $ARCaP_E$, and $ARCaP_M$ cells. 28S rRNA RT-PCR was done to assess the quality of the cDNA and ensure equal amounts of cDNA used in the PCRs and β-actin was used as a loading control for the whole-cell lysates. *B,* representative pictures from tissue microarray of immunohistochemical staining of ZEB1 in normal and prostate cancer tissues. The normal age-matched tissues (*panel 1*) were compared with low Gleason (≤6; *panel 2*) and high Gleason (≥8) prostate cancer tissues (*panel 3*). Photos were taken under ×200 magnification. *C,* summary of differential ZEB1 expression between normal and prostate cancer tissues. Fisher's exact test was used to analyze the association of ZEB1 expression with Gleason score. $P \leq 0.001$.

luminal origin derived from ascitic fluid of a patient with metastatic prostate cancer. The $ARCaP_E$ and $ARCaP_M$ cells were derived from single-cell dilution of the ARCaP cells. This model represents a lethal form of human prostate cancer with increased prostate-specific antigen and the ability to invade and metastasize aggressively to bone and adrenal gland. When grown in two-dimensional culture, $ARCaP_E$ cells exhibit a cuboidal, epithelial morphology with high expression of epithelial markers, such as cytokeratin 18 and E-cadherin (36). The lineage-derived $ARCaP_M$ cells have a spindle-shaped mesenchymal morphology and phenotype, with high expression of vimentin and N-cadherin. These cells have decreased cell adhesion and increased metastatic propensity to bone and adrenal glands (36). The morphologic and phenotypic changes observed in the $ARCaP_M$ cells resemble that of cells undergoing EMT. To confirm this observation, we analyzed the expression of ZEB1, a transcriptional repressor involved in EMT.

Previous reports have shown that ZEB1 expression is constitutively elevated in several malignancies, including breast, lung, ovarian, and colorectal cancers (8, 13–15, 37). However, to date, ZEB1 expression has not been investigated in prostate cancer. To evaluate the relationship between ZEB1 and prostate cancer malignancy *in vitro*, we analyzed the gene and protein expression of ZEB1 by semiquantitative reverse transcription-PCR (RT-PCR) and Western blot analyses, respectively, among a panel of prostate cancer cells (LNCaP, a poorly tumorigenic cell line, its bone-derived subline, C4-2B, and the metastatic cell lines DU-145, PC-3, $ARCaP_E$, and $ARCaP_M$). A representative pattern of expression is shown in Fig. 1*A*. The expression of ZEB1 was variable among the cell lines tested. ZEB1 mRNA and protein expression were observed primarily in the highly aggressive, metastatic cell lines DU-145 and $ARCaP_E$ and, to a greater extent, in $ARCaP_M$ cells (Fig. 1*A*).

We next examined the expression of ZEB1 in normal human prostate tissue and in prostate carcinomas with low or high Gleason score by immunohistochemistry to investigate whether there is differential expression between benign and malignant prostate tissues. As shown in Fig. 1*B*, there was almost undetectable ZEB1 protein expression in the normal prostate (*panel 1*), weak to moderate expression in tumors with low Gleason scores, and strong, intense expression in tumors with high Gleason scores (*panels 2* and *3*). Statistical analysis revealed that overall ZEB1 expression level was strongly correlated with Gleason scores ($P < 0.001$; Fig. 1*C*) and tumors with high Gleason scores (≥ 8) exhibited significantly higher immunostaining for ZEB1 compared with tumors with lower Gleason scores (≤ 6), summarized in Fig. 1*C*. These results indicate that ZEB1 protein expression is increased in prostate cancer tissue compared with normal tissue and its expression is correlated with tumor grade and aggressiveness.

Enhanced IGF-I signaling elevates ZEB1 expression *in vitro*. Many stimulatory, soluble factors, such as epidermal growth factor and IGF-I, can confer EMT in cancer cells by increasing the expression of transcription factors that promote this process (9). ZEB1 has been shown to down-regulate E-cadherin and promote EMT in breast cancer (8, 37); however, the upstream factor(s) that induces the expression of ZEB1 has not been identified. Various lines of evidence suggest the involvement of the IGF-I axis in the development of prostate cancer (25, 38). We determined by immunoblot analysis that although both ARCaP cell lines express the IGF-IRβ, the more aggressive $ARCaP_M$ cells have a 2-fold higher phosphorylated IGF-IRβ (Fig. 2*A*). In addition, using the conditioned medium from $ARCaP_E$ and $ARCaP_M$ cells, we determined that both cell lines secrete barely detectable levels of IGF-I, suggesting that IGF-I signaling occurs in a paracrine manner (data not shown). To identify IGF-I as an upstream regulator of EMT in prostate cancer cells through ZEB1, $ARCaP_E$ and $ARCaP_M$ cells were treated with vehicle or physiologic concentrations of IGF-I (100 or 200 ng/mL) for 6 h, the time point that induced the highest ZEB1 expression (Fig. 2*C*), followed by RT-PCR and immunoblot analysis to quantify the mRNA and protein expression of ZEB1, respectively. As shown in Fig. 2*B*, ZEB1 mRNA was up-regulated 6.3- and 11.3-fold in a ligand-dependent manner in response to 100 and 200 ng/mL of recombinant IGF-I in $ARCaP_E$ cells. The

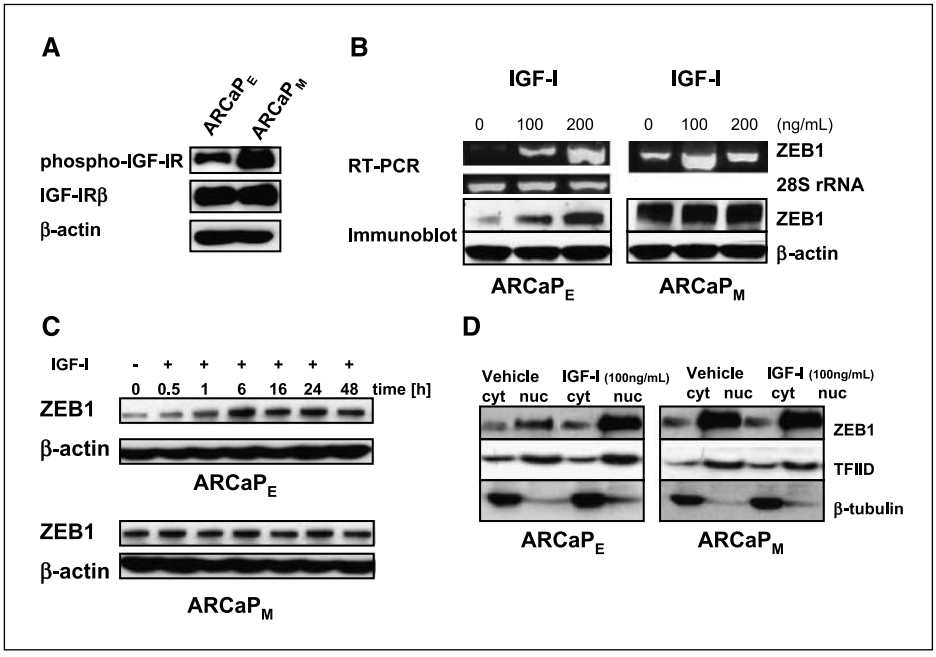

Figure 2. IGF-I induces ZEB1 expression in $ARCaP_E$ cells. *A,* immunoblot analysis of phosphorylated and total IGF-IRβ expression in $ARCaP_E$ and $ARCaP_M$ whole-cell lysates. *B,* $ARCaP_E$ and $ARCaP_M$ were treated with 100 or 200 ng/mL of recombinant IGF-I for 6 h followed by RT-PCR and immunoblot analysis to monitor ZEB1 mRNA and ZEB1 protein in whole-cell lysates. *C,* $ARCaP_E$ and $ARCaP_M$ cells were cultured with recombinant IGF-I (100 ng/mL) for the indicated time points. *D,* cytosolic and nuclear fractions were isolated by sequential extraction. As a loading control for the nuclear extracts, TFIID was used, and β-tubulin for the cytosolic fraction. The images are a representation of three independent experiments.

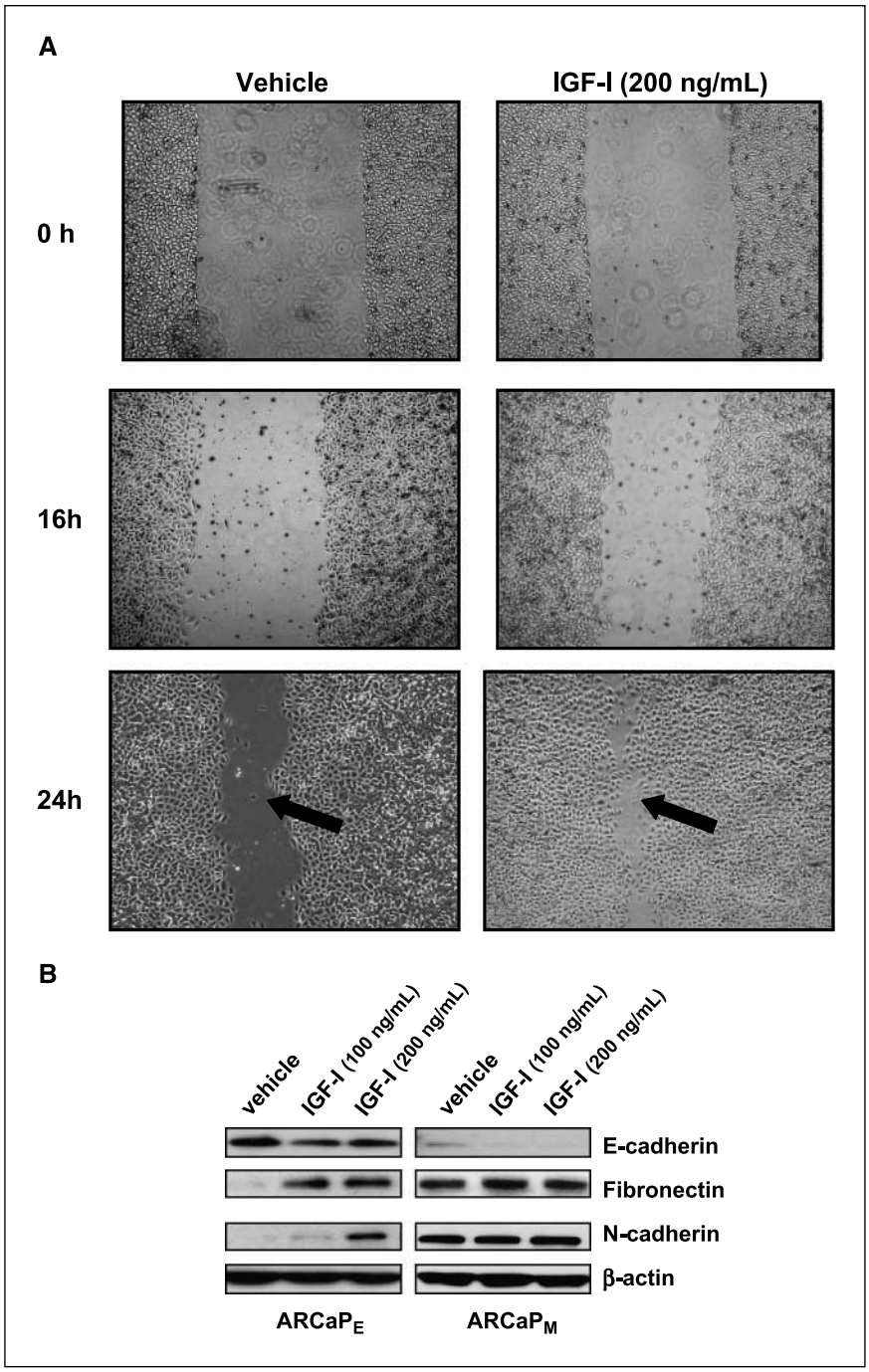

Figure 3. IGF-I enhances ARCaP$_E$ migratory properties. *A,* representative results of the scratch wound assay. *Arrows,* differential migration rate. Recombinant human IGF-I enhances the motility of ARCaP$_E$ cells. Photos were taken at ×100 magnification. *B,* immunoblot analysis of ARCaP$_E$ and ARCaP$_M$ cells treated with recombinant IGF-I for 10 d.

immunoblot results correlate with the RT-PCR data in that ZEB1 protein expression increased in response to IGF-I treatment in ARCaP$_E$ cells. The protein expression of ZEB1 in ARCaP$_M$ cells is constitutively elevated and therefore was not further modulated by IGF-I. By subcellular fractionation, we observed in ARCaP$_E$ cells that, in response to IGF-I, there is a 2-fold increase of ZEB1 in the nucleus compared with the control (Fig. 2*B*). However, ARCaP$_M$ cells exhibit high ZEB1 nuclear expression in both control and IGF-I–treated cells, which is consistent with the high constitutive levels observed in Fig. 2*B*. To examine the functional significance of IGF-I on prostate cancer cell migration, a major event that occurs during EMT, we used an *in vitro* scratch wound assay. Recombinant IGF-I increased the ability of the ARCaP$_E$ cells to migrate into the wound dose dependently compared with the control (Fig. 3*A*). These data correlate with the increased expression of the mesenchymal markers fibronectin and N-cadherin in response to IGF-I after 10 days of exposure. In the ARCaP$_M$ cells, IGF-I did not increase the protein expression of the mesenchymal markers; however, there was a reduction in E-cadherin expression (Fig. 3*B*).

ZEB1 expression is MEK dependent *in vitro*. To dissect the mechanism(s) of intracellular signaling for ZEB1 activation in prostate cancer cells, we examined the potential role of PI3K/Akt and MEK signaling. PI3K does not seem to play a major role, as treatment with the chemical inhibitor LY294002 did not suppress

ZEB1 expression in the ARCaP cells (data not shown). $ARCaP_E$ has a lower level of activated ERK compared with $ARCaP_M$ cells, and treatment with IGF-I increased the phosphorylation of ERK to levels comparable with the mesenchymal cell line (Fig. 4*A*). To determine if ERK activation is involved in ZEB1 expression, $ARCaP_M$ cells were treated with the chemical inhibitor to MEK/ERK, U0126, for 48 h before IGF-I stimulation for 6 h. As noted previously, IGF-I treatment in these cells did not increase ZEB1 expression in $ARCaP_M$ cells but inhibition of MEK/ERK by U0126 reduced ZEB1 expression (Fig. 4*B*). This suggests that expression of ZEB1 is mediated through the MAPK pathway in $ARCaP_M$. In addition to ZEB1 suppression, MEK/ERK inhibition lowered β-catenin expression and increased in E-cadherin expression by 16-fold. Interestingly, there was no suppression of the mesenchymal markers fibronectin and vimentin, suggesting that other pathways may contribute to the sustained maintenance of EMT gene expression changes. In addition, suppression of MEK for 48 h with U0126 resulted in a morphologic switch of mesenchymal phenotype to an epithelial phenotype in $ARCaP_M$ cells (Fig. 4*C*). Treatment with the MEK/ERK inhibitor in $ARCaP_E$ cells reduced the ZEB1 expression and treatment with IGF-I partially restored ZEB1 (Fig. 4*B*). Similar to the $ARCaP_M$ cells, inhibition of MEK/ERK results in suppression of β-catenin but did not modulate the endogenously low levels of the mesenchymal markers fibronectin and vimentin. In addition, suppression of MEK/ERK did not enhance the epithelial morphology of these cells.

ZEB1 represses E-cadherin in human prostate cancer cells. Loss of E-cadherin expression in human cancers is frequently associated with increased cell migration, cell invasion, and ultimately poor prognosis (39, 40). $ARCaP_M$ cells were transfected with either ZEB1 siRNA to reduce endogenous ZEB1 expression or lamin A siRNA as an unrelated control and the morphologic changes were monitored for 6 days after transfection. We observed that the cells transfected with ZEB1 siRNA were less spindle shaped compared with the control and exhibited a more epithelial morphology (Fig. 5*A*). To determine whether molecular alterations associated with EMT correlate with the morphologic changes observed, we conducted immunoblot analysis of downstream proteins in $ARCaP_M$ cells in which ZEB1 is inactivated. Immunoblotting of whole-cell lysates showed approximately 80% to 90% decrease of ZEB1 protein levels on treatment with the ZEB1-specific siRNA (Fig. 5*B*). Expression of N-cadherin and fibronectin, critical markers associated with cell migration, along with β-catenin was decreased in the ZEB1 siRNA-transfected cells. E-cadherin expression was highly induced in the transfected cells, and morphologically, there was a dramatic change in the cell phenotype consistent with a mesenchymal to epithelial transition (MET). Because loss of E-cadherin is one of the critical features of EMT and its membrane localization indicates its biological function, we conducted immunofluorescent staining in $ARCaP_M$ cells. Immunofluorescence revealed that, on ZEB1 inhibition, E-cadherin relocalized to the plasma membrane and its expression was strongly enriched at the areas of cell-cell contact in $ARCaP_M$ (Fig. 5*C*). To further study whether ZEB1 can modulate EMT markers, we overexpressed ZEB1 in $ARCaP_E$ cells. Immunoblot analysis showed that transiently transfecting these cells with a ZEB1 expression vector resulted in an increase in N-cadherin, with concomitant decrease of E-cadherin compared with the control transfected cells (Fig. 5*B*). Taken together, ZEB1 was sufficient to induce molecular changes associated with EMT in prostate cancer cells.

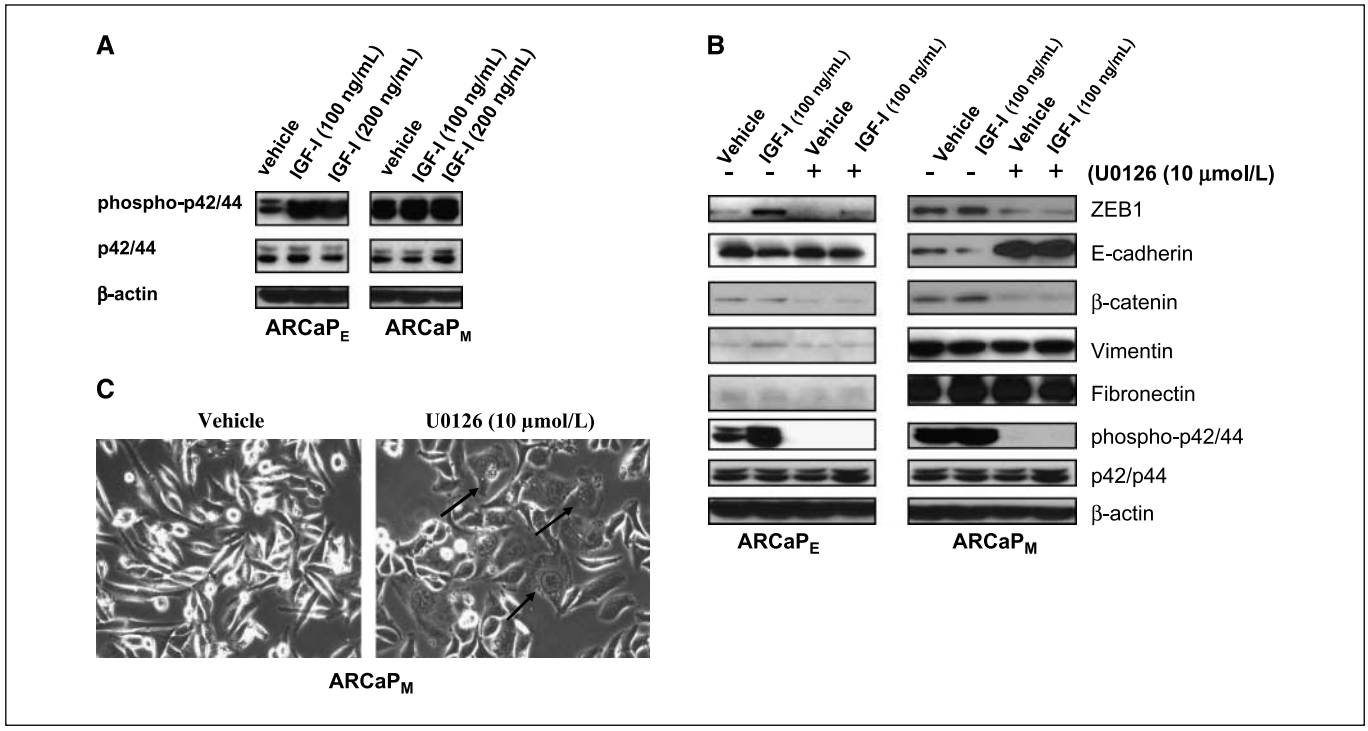

Figure 4. ZEB1 expression is MEK/ERK dependent. *A,* immunoblot of whole-cell lysates from $ARCaP_E$ and $ARCaP_M$ cell monitoring the endogenous phosphorylated and total ERK. The cells were treated with vehicle or recombinant IGF-I for 1 h. *B,* immunoblot analysis of $ARCaP_E$ and $ARCaP_M$ cells that were treated with the MEK/ERK inhibitor U0126 (10 μmol/L) or vehicle for 48 h followed by IGF-I treatment for 6 h. *C,* $ARCaP_M$ cells treated with the MEK/ERK inhibitor for 48 h resemble an epithelioid morphology. Photos were taken at ×100 magnification.

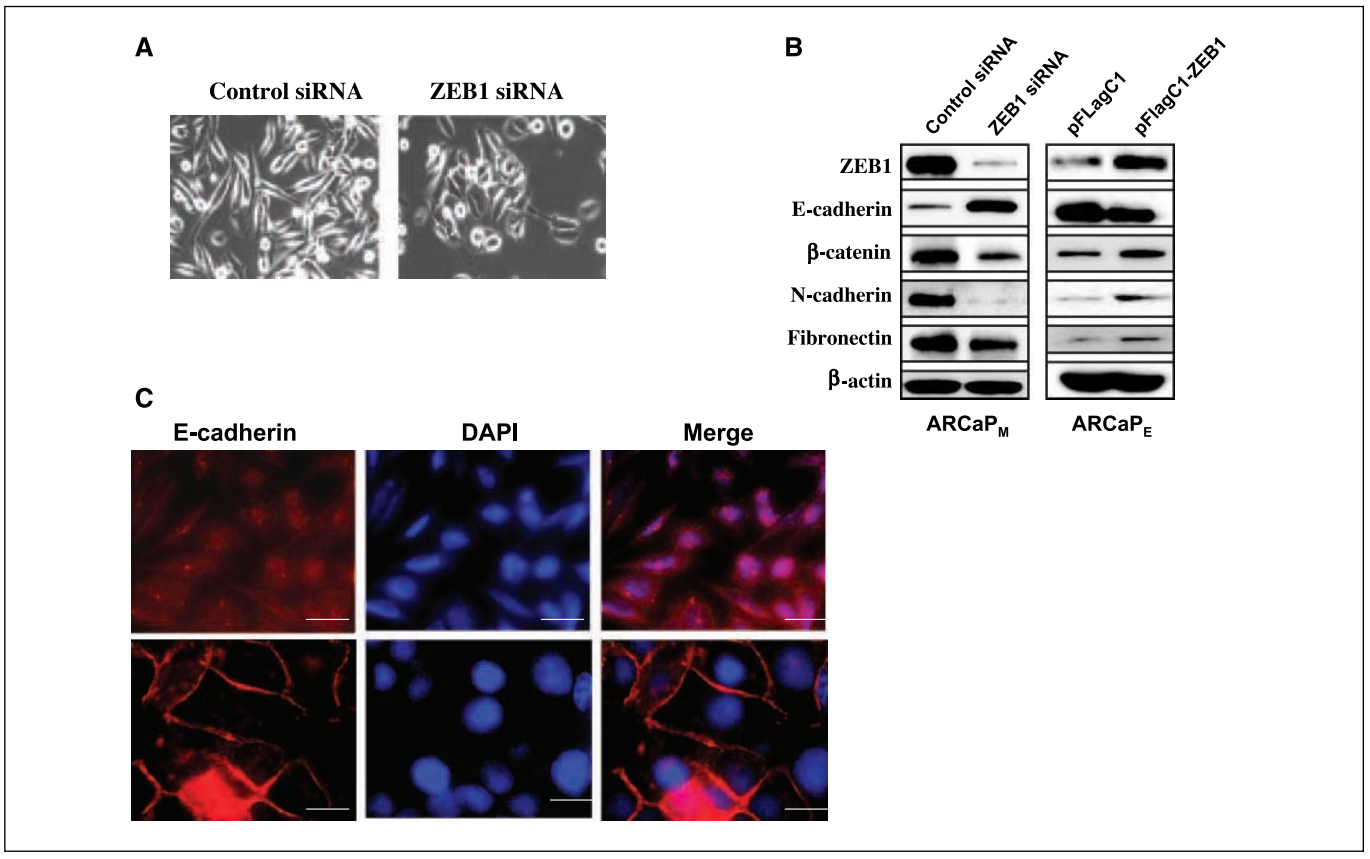

Figure 5. ZEB1 inhibition modulates EMT markers in prostate cancer cells. *A,* morphologic changes induced by ZEB1 inhibition in ARCaP$_M$ cells grown in two-dimensional culture. Photos were taken at ×100 magnification. *B,* immunoblot analysis. ARCaP$_M$ transfected with cyclophilin B siRNA or ZEB1 siRNA. ARCaP$_E$ cells were transiently transfected with either a control plasmid (pFlagC1) or ZEB1 expression vector (pFlagC1-ZEB1). Forty-eight hours after transfection, the whole-cell lysates were probed with the specific antibodies. *C,* immunofluorescence staining of E-cadherin in ARCaP$_M$ cells transfected with either cyclophilin B siRNA or ZEB1 siRNA. *Bar,* 100 μm. *DAPI,* 4′,6-diamidino-2-phenylindole.

ZEB1 promotes prostate cancer cell migration and invasion. The increased membrane expression of E-cadherin in response to ZEB1 blockade led us to examine the effect on cell migration, a hallmark of EMT. As shown in Fig. 6*A*, the migration rate of ARCaP$_M$ transfected with ZEB1 siRNA cells was reduced compared with the control transfectants, indicating that ZEB1 is an important mediator of ARCaP$_M$ cell migration. For cancer cells to invade surrounding tissue, the cells must degrade the underlying basement membrane. To determine a role for ZEB1 in prostate cancer cell invasion, we evaluated the ability of ARCaP$_M$ cells to invade the extracellular matrix. Cells were transfected with ZEB1 siRNA or control siRNA and seeded onto a filter that was coated with Matrigel. Strikingly, suppression of endogenous ZEB1 expression by siRNA resulted in significant inhibition of prostate cancer cell invasion, resulting in an 8-fold reduction in the ability of the cells to invade through Matrigel compared with the control siRNA-treated cells (Fig. 6*B*). Collectively, these results suggest that ZEB1 down-regulation in prostate cancer cells promotes phenotypic changes associated with EMT as shown by alterations in epithelial and mesenchymal protein expression and mediates cell migration and invasion.

Discussion

ZEB1 has been identified as a critical regulator of EMT and ultimately functions as a metastasis promoter in a variety of cancer types (8, 13–15, 37); however, the role ZEB1 plays in prostate cancer EMT has yet to be elucidated. In this study, we used the human prostate cancer EMT model, ARCaP. The ARCaP$_E$ cell line has a characteristic epithelial phenotype, whereas the ARCaP$_M$ cells exhibit a mesenchymal phenotype. We were interested in studying the molecular mechanisms governing ZEB1 activation and expression in these cells. We show that IGF-I is a key ligand that promotes prostate cancer cells with an epithelial phenotype to become more mesenchymal in part by up-regulating ZEB1. Both ARCaP$_E$ and ARCaP$_M$ cells secrete low levels of IGF-I. These data correlate with previous reports illustrating that although the mRNA of IGF-I was detected in prostate cancer cell lines, they did not secrete an immunoreactive level of IGF-I into their conditioned medium compared with prostate stromal cells (32, 41). This suggests that prostate cancer cells use IGF-I secreted from the local stroma to enhance their migratory and invasive properties. By RT-PCR and immunoblot analysis, IGF-I was found to induce ZEB1 expression in ARCaP$_E$ cells. These findings are consistent with a previous report in which IGF-I induced the gene expression of Twist, a basic loop helix transcription factor, known to promote EMT (42). In the more aggressive ARCaP$_M$ cells, ZEB1 is constitutively expressed, as evidenced by immunoblot analysis.

There are several zinc finger transcription factors, including Snail and Slug, which have been described as E-cadherin repressors (43, 44). ZEB1 has also been linked to E-cadherin repression,

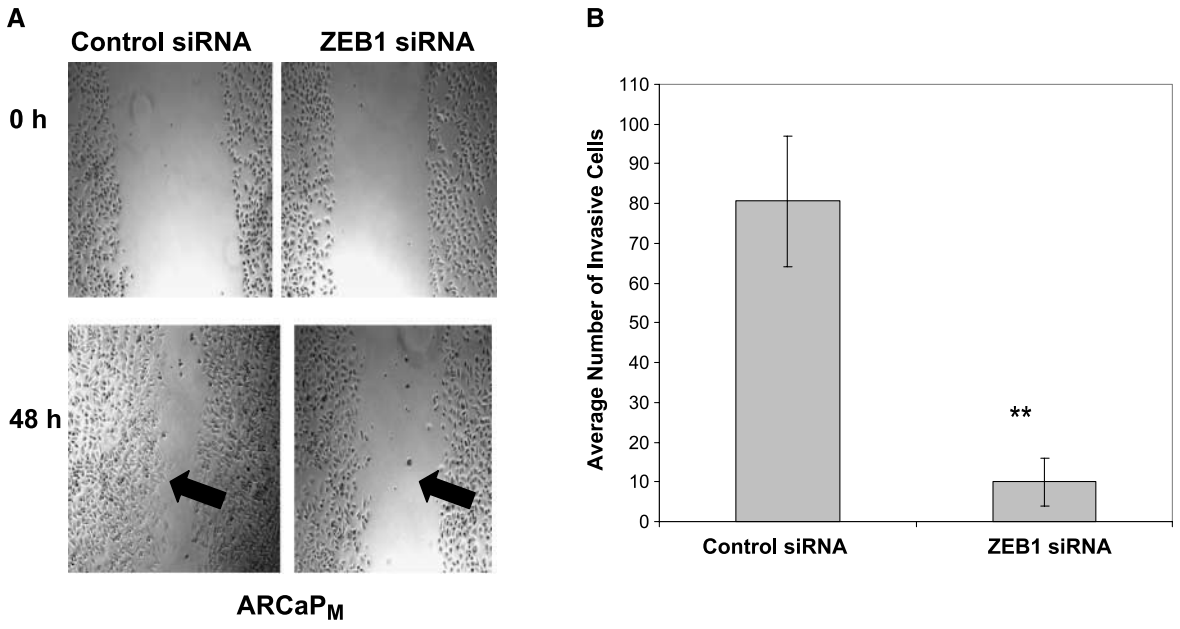

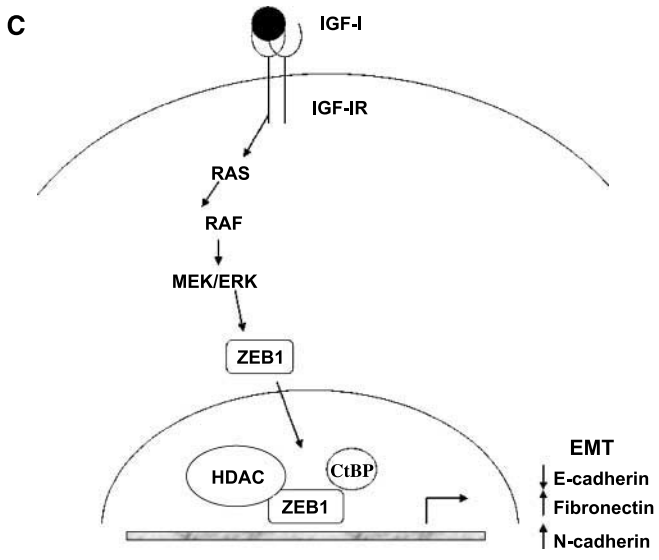

Figure 6. ZEB1 promotes ARCaP$_M$ cell migration and invasion. *A,* ARCaP$_M$ cells were transfected with either lamin A siRNA or ZEB1 siRNA, and 48 h later, the cells were wounded. Photos were taken at ×100 magnification. *B,* ARCaP$_M$ cells transfected with ZEB1 siRNA were plated on Matrigel-coated filters and the invasive cells were fixed, stained with crystal violet, and counted. The data presented are a representation of three independent experiments. *C,* proposed model for ZEB1 activation by IGF-I. IGF-I activates MEK/ERK, which enhances ZEB1 expression in prostate cancer cells. This results in decreased E-cadherin expression and concomitant increase in mesenchymal markers, such as fibronectin and N-cadherin. *HDAC,* histone deacetylase.

thereby enhancing the ability of the cancer cells to migrate to distal sites (7, 17). Down-regulation of ZEB1, through the use of siRNA, restored expression of the epithelial marker E-cadherin and concomitant loss of the mesenchymal markers β-catenin, N-cadherin, and fibronectin in ARCaP$_M$ cells. Frequently in cancers, loss of E-cadherin coincides with up-regulated expression of mesenchymal cadherins, such as N-cadherin (cadherin switch), raising the possibility that not only the loss of E-cadherin but also the gain of N-cadherin function and other mesenchymal markers may contribute to tumor progression (19). The biological significance of ZEB1 in prostate cancer EMT was shown by the fact that ZEB1 blockade suppressed cell motility and invasive abilities *in vitro*, concurrent with the observed molecular changes. These results support other studies conducted in colorectal cancer cells in which transiently reducing ZEB1 expression by siRNA decreased the invasiveness of these cells (15). Untransfected and control transfected SW480 colorectal cancer cells grow in a mesenchyme-like phenotype, characterized by loosely attached cells, lacking membranous E-cadherin and strongly accumulating nuclear β-catenin (15). ZEB1 knockdown changed the cell phenotype resembling a MET (15). In high-grade, aggressive uterine tumors, ZEB1 is aberrantly expressed and uterine cancer cells that have metastasized have up-regulated ZEB1 expression (13). In addition, a recent report implied ZEB1 in E-cadherin repression in lung cancer biology (14). Nuclear factor-κB represses E-cadherin expression and enhances EMT of mammary epithelial cells by activation of ZEB1 (37). Similar to colorectal cancer cells, knockdown of ZEB1 in MCF-10A breast cancer cells reduced E-cadherin expression and reversed the mesenchymal phenotype.

Our data suggest that MEK/ERK is an upstream factor of ZEB1 activation in prostate cancer cells *in vitro*. IGF-I has been shown to activate the MEK1/2 MAPK pathway in various cancer cells (45, 46), and we show in $ARCaP_E$ and $ARCaP_M$ cells that ZEB1 expression is MEK dependent. Pharmacologic inhibition of ERK signaling has been shown to decrease invasion or inhibit specific biochemical changes consistent with EMT (47, 48). Although ERK inhibition lowered ZEB1 protein expression and restored expression of the epithelial marker E-cadherin, it did not significantly down-regulate expression of mesenchymal markers in $ARCaP_M$ cells. These results are consistent with previous reports (48, 49), suggesting that the failure to completely reverse EMT may be caused by irreversible changes induced by enhanced ERK activation or to ERK-independent pathways that are sufficient to maintain the mesenchymal phenotype. Based on our results, we propose a model (Fig. 6*C*) in which IGF-I activation of ZEB1 is MEK/ERK dependent in prostate cancer cells.

In summary, increasing evidence implicates ZEB1 activation in promoting the invasiveness of prostate cancer. ZEB1 functions by down-regulating the expression of E-cadherin in several cancer types, including uterine (13), lung (14), colorectal (15), and breast (8, 37), thereby increasing the migratory and invasive properties of the cells. The present study suggests that the aberrant expression of ZEB1 occurs in part due to IGF-I, which is a factor known to be elevated in the serum of patients with aggressive prostate cancer (26, 27). The activated ZEB1 is then able to promote epithelial prostate cancer cells to exhibit a mesenchymal phenotype. The molecular mechanisms responsible for ZEB1 up-regulation warrant further investigation in defining cross-talk with other signaling pathways in prostate cancer metastasis.

Acknowledgments

Received 7/6/2007; revised 12/11/2007; accepted 2/6/2008.

Grant support: Department of Defense Consortium grant DAMD 170320033 (J.W. Simons), National Cancer Institute Center of Cancer Nanotechnology Excellence grant CA119338 (R.M. O'Regan and J.W. Simons), Wilbur and Hilda Glenn Foundation (R.M. O'Regan), Georgia Cancer Coalition (R.M. O'Regan), and PO1 CA098912 (Leland W.K. Chung).

The costs of publication of this article were defrayed in part by the payment of page charges. This article must therefore be hereby marked *advertisement* in accordance with 18 U.S.C. Section 1734 solely to indicate this fact.

References

1. Keller E, Zhang J, Copper C, Smith P, McCauley L. Prostate carcinoma skeletal metastases: cross-talk between tumor and bone. Cancer Metastasis Rev 2001; 20:73–6.
2. Theiry J. Epithelial-mesenchymal transitions in tumor progression. Nat Rev 2002;4:442–54.
3. Vincent-Salomon A, Theiry JP. Epithelial-mesenchymal transition in breast cancer development. Breast Cancer Res 2003;5:101–6.
4. Bindels S, Mestdagt M,Vandewalle C, et al. Regulation of vimentin by SIP1 in human epithelial breast tumor cells. Oncogene 2006;25:4975–85.
5. Luo Y, He DL, Ning L, et al. Over-expression of hypoxia-inducible factor-1α increases the invasive potency of LNCaP cells *in vitro*. Br J Urol 2006;98: 1315–19.
6. Guaita S, Puig I, Francí C, et al. Snail induction of epithelial to mesenchymal transition in tumor cells is accompanied by MUC1 repression and ZEB1 expression. J Biol Chem 2002;277:39209–16.
7. Kwok W, Ling M, Lee T, et al. Upregulation of TWIST in prostate cancer and its' implication as a therapeutic target. Cancer Res 2005;65:5153–62.
8. Eger A, Aigner K, Sonderegger S, et al. ΔEF1 is a transcriptional repressor of E-cadherin and regulates epithelial plasticity in breast cancer cells. Oncogene 2005;24:2375–85.
9. Peinado H, Olmeda D, Cano A. Snail, ZEB and bHLH factors in tumour progression: an alliance against the epithelial phenotype? Nat Rev 2007;7:415–28.
10. Postigo A, Depp J, Taylor J, Kroll K. Regulation of Smad signaling through a differential recruitment of coactivators and corepressors by ZEB proteins. EMBO J 2003;22:2453–62.
11. van Grunsven L, Taelman V, Michiels C, Opdecamp K, Huylebroeck D, Bellefroid EJ. δEF1 and SIP1 are differentially expressed and have overlapping activities during *Xenopus* embryogenesis. Dev Dyn 2006; 235:1491–500.
12. Postigo A, Dean D. Differential expression and function of members of the zfh-1 family of zinc finger/homeodomain repressors. Proc Natl Acad Sci U S A 2000;97:6391–6.
13. Spoelstra N, Manning N, Higashi Y, et al. The transcription factor ZEB1 is aberrantly expressed in aggressive uterine cancers. Cancer Res 2006;66: 3893–902.
14. Ohira T, Gemmill R, Ferguson K, et al. WNT7a induces E-cadherin in lung cancer cells. Proc Natl Acad Sci U S A 2003;100:10429–34.
15. Spaderna S, Schmalhofer O, Hlubek F, et al. A transient, EMT-linked loss of basement membranes indicates metastasis and poor survival in colorectal cancer. Gastroenterology 2006;131:830–40.
16. Grooteclaes M, Frisch S. Evidence for a function of CtBP in epithelial gene regulation and anoikis. Oncogene 2000;19:3823–8.
17. Chinnadurai G. CtBP, an unconventional transcriptional corepressor in development and oncogenesis. Mol Cell 2002;9:213–24.
18. Olmeda D, Jorda M, Peinado H, Fabra A, Cano A. Snail silencing effectively suppresses tumor growth and invasiveness. Oncogene 2007;26:1862–74.
19. Herzig M, Savarese F, Novatchkova M, Semb H, Christofori G. Tumor progression induced by the loss of E-cadherin independent of β-catenin/Tcf-mediated Wnt signaling. Oncogene 2007;25:2290–8.
20. Aigner K, Dampier B, Descovich L, et al. The transcription factor ZEB1 (δEF1) promotes tumour cell dedifferentiation by repressing master regulators of epithelial polarity. Oncogene 2007;26:6979–88.
21. Postigo A, Dean D. ZEB, a vertebrate homolog of *Drosophila* Zfh-1, is a negative regulator of muscle differentiation. EMBO J 1997;16:3935–43.
22. Yu H, Rohan T. Role of the insulin-like growth factor family in cancer development and progression. J Natl Cancer Inst 2000;92:1472–81.
23. Samani A, Yakar S, LeRoith D, Brodt P. The role of the IGF system in cancer growth and metastasis: overview and recent insights. Endocr Rev 2007;28:20–47.
24. Adhami VM, Afaq F, Mukhtar H. Insulin-like growth factor axis as a pathway for cancer prevention. Clin Cancer Res 2006;12:5611–4.
25. Pollak M, Schernhammer E, Hankinson S. Insulin-like growth factors and neoplasia. Nat Rev 2004;4:505–18.
26. Khosravi J, Diamandi A, Mistry J, Scorilas A. Insulin-like growth factor I (IGF-I) and IGF-binding protein in benign prostatic hyperplasia and prostate cancer. J Clin Endocrinol Metab 2001;86:694–9.
27. Hsing A, Chua S, Gao Y, et al. Prostate cancer risk and serum levels of insulin and leptin: a population-based study. J Natl Cancer Inst 2001;93:783–9.
28. Ibrahim Y, Yee D. Insulin-like growth factor-I and cancer risk. Growth Horm IGF Res 2004;14:261–9.
29. Lonning PE, Helle S. IGF-I and breast cancer. Novartis Found Symp 2004;262:205–12.
30. Wu J, Haugk K, Woodke L, Nelson P, Coleman I, Plymate S. Interaction of IGF signaling and the androgen receptor in prostate cancer progression. J Cell Biochem 2006;99:392–401.
31. Krueckl S, Sikes R, Edlund N, et al. Increased insulin-like growth factor I receptor expression and signaling are components of androgen-independent progression in a lineage-derived prostate cancer progression model. Cancer Res 2004;64:8620–9.
32. Kawada M, Inoue H, Masuda T, Ikeda D. Insulin-like growth factor I secreted from prostate stromal cells mediates tumor-stromal cell interactions of prostate cancer. Cancer Res 2006;66:4419–25.
33. Sterns M, Tran J, Francis M, Zhong H, Sell C. Activated Ras enhances insulin-like growth factor I induction of vascular endothelial growth factor in prostate epithelial cells. Cancer Res 2005;65: 2085–8.
34. Miyamoto S, Nakamura M, Shitara K, et al. Blockade of paracrine supply of insulin-like growth factors using neutralizing antibodies suppresses the liver metastasis of human colorectal cancers. Clin Cancer Res 2005;11: 3494–502.
35. Irie H, Pearline R, Grueneberg D, et al. Distinct roles of Akt1 and Akt2 in regulating cell migration and epithelial-mesenchymal transition. J Cell Biol 2005;171: 1023–34.
36. Xu J, Wang R, Xie Z, et al. Prostate cancer metastasis: role of the host microenvironment in promoting epithelial to mesenchymal transition and increased bone and adrenal gland metastasis. Prostate 2006;66: 1664–73.
37. Chua H, Bhat-Nakshatri P, Clare S, Morimiya A, Badve S, Nakshatri H. NF-κB represses E-cadherin expression and enhances epithelial to mesenchymal transition of mammary epithelial cells: potential involvement of ZEB-1 and ZEB-2. Oncogene 2007;26: 711–24.
38. Damon S, Plymate S, Carroll J, et al. Transcriptional regulation of insulin-like growth factor-I receptor gene expression in prostate cancer cells. Endocrinology 2001; 142:21–7.
39. Christofori G, Semb H. The role of the cell-adhesion molecule E-cadherin as a tumor-suppressor gene. Trends Biochem Sci 1999;24:73–6.
40. Bremnes RM, Veve R, Hirsch FR, Franklin WA. The E-cadherin cell-cell adhesion complex and lung cancer invasion, metastasis, and prognosis. Lung Cancer 2002; 36:115–24.

41. Kimura G, Kasuya J, Giannini S, et al. Insulin-like growth factor (IGF) system components in human prostatic cancer cell lines: LNCaP, DU-145 and PC-3 cell. Int J Urol 1996;3:39–46.
42. Dupont J, Fernandez A, Glackin C, Helman L, LeRoith D. Insulin-like growth factor-I (IGF-I)-induced twist expression is involved in the anti-apoptotic effects of the IGF-1 receptor. J Biol Chem 2001;276:73–6.
43. Barallo-Gimeno A, Nieto MA. The Snail genes as inducers of cell movement and survival: implications in development and cancer. Development 2005;132:3151–61.
44. Come C, Magnino F, Bibeau F, et al. Snail and slug play distinct roles during breast carcinoma progression. Clin Cancer Res 2006;12:5395–402.
45. Burroughs K, Oh J, Barrett J, DiAugustine R. Phosphatidylinositol 3-kinase and Mek1/2 are necessary for insulin-like growth factor vascular endothelial growth factor synthesis in prostate epithelial cells: a role for HIF-Iα. Mol Cancer Res 2003;1:312–22.
46. Suzuki K, Takahashi K. Anchorage-independent activation of mitogen-activated protein kinase through phosphatidylinositol-3 kinase by insulin-like growth factor I. Biochem Biophys Res Commun 2000;272:111–5.
47. Janda E, Lehmann K, Killisch I, et al. TGFβ cooperatively regulate epithelial cell plasticity and metastasis: dissection of Ras signaling pathways. J Cell Biol 2002;156:299–313.
48. Grande M, Franzen A, Karlsson J, Ericson L, Heldin N, Nilsson M. Transforming growth factor-β and epidermal growth factor synergistically stimulate epithelial to mesenchymal transition (EMT) through a MEK-dependent mechanism in primary cultured pig thyrocytes. J Cell Sci 2002;115:4227–36.
49. Khoury H, Naujokas M, Zuo D, et al. HGF converts ErbB2/Neu epithelial morphogenesis to cell invasion. Mol Biol Cell 2005;16:550–61.